The response function of a two-dimensional electron gas in a unidirectional spatially periodic magnetic modulation



1996 J. Phys.: Condens. Matter 8 6019

(http://iopscience.iop.org/0953-8984/8/33/010)

J. Phys.: Condens. Matter **8** (1996) 6019–6033. Printed in the UK

# The response function of a two-dimensional electron gas in a unidirectional spatially periodic magnetic modulation

S M Stewart and C Zhang

Department of Physics, University of Wollongong, NSW 2522, Australia

Received 26 March 1996, in final form 7 June 1996

**Abstract.** The dynamical dielectric response function and collective excitations of a two-dimensional electron gas under a perpendicular magnetic field and in the presence of an additional weak unidirectional spatially modulated periodic *magnetic* field are calculated within the random-phase approximation. It is found that the dynamical dielectric response function is not only broadened by the additional magnetic modulation, but it also contains a series of subsingularities at the band edges. Such broadening of the response function is also found to modify the magnetoplasmon modes of such a system over their unmodulated counterpart. The origin of the new subsingularities is attributed to the magnetic modulation-induced broadening of the energy spectrum. This broadening, being non-uniform, leads to the reintroduction of particle–hole excitations into the dielectric response function. Such fine structures at the band edges are similar in appearance to those recently reported for the case of a weak unidirectional spatially modulated periodic *electric* potential though however the former may be up to about an order of magnitude larger in bandwidth compared to those seen for the *electric* case when equal modulation strengths are considered. It is therefore proposed that these new predicted fine structures should be more readily observed in far-infrared spectroscopy experiments over their *electric* counterpart.

## 1. Introduction

Recently there has been considerable interest, both theoretically [1–7] and experimentally [8–10], in a two-dimensional electron gas (2D EG) system in a uniform magnetic field and under an additional one-dimensional periodic spatial *magnetic* modulation. Such work has followed on from its analogue system, that of a 2D EG system in a uniform magnetic field and under an additional one-dimensional periodic spatial *electric* potential modulation, which has to date been extensively studied [11–15].

Most work on the magnetically modulated system has been for *weakly* modulated systems (i.e. $B_m \ll B_0$ where $B_m$ is the amplitude of the magnetic modulation while $B_0$ is the strength of the uniform magnetic field) where the transport properties in the static limit have been studied. Little work has been done on the dynamical response properties of such systems.

In this paper we investigate the dynamical response function and collective excitations of a 2D EG under a uniform perpendicular magnetic field and in the presence of an additional one-dimensional periodic spatial magnetic modulation which is *weak*. Following on from earlier work for the analogue *electric* case [14, 15], where it was found that the response function is not only broadened by the additional *electric* modulation but contained a series of van Hove subsingularities at the band edges, we show that such behaviour is reciprocated in the *magnetic* case. Moreover it is found that these van Hove subsingularities at the

0953-8984/96/336019+15$19.50  

band edges differ from their *electric* counterpart in that they may be considerably more broadened in bandwidth for equal modulation amplitude strengths (i.e. $V_0 = \hbar\omega_m$, where $V_0$ is the amplitude of the *electric* modulation while we have written $\omega_m = eB_m/m_b$ in analogy to the cyclotron frequency $\omega_c$, $m_b$ being the effective band mass of an electron). This is a feature which experimentally will be advantageous compared with that of the *electric* case since being larger in bandwidth they should be more readily seen in an optical experiment. For the collective excitations of the system we confine ourselves to the study of only the principal magnetoplasmon mode. Here it is found that the principal magnetoplasmon mode, being dependent for its behaviour on the behaviour of the dynamical dielectric response function, is modified due to the induced broadening of the response function brought about by the additional *magnetic* modulation.

In section 2 we give the one-electron Hamiltonian describing our system and use it to calculate, perturbatively, the energy spectrum. We also present here results for the density of states (DOS) and zero-temperature chemical potential. In section 3 we present results for the response function which are compared with the *electric* case while in section 4 the collective excitations are studied. Section 5 is devoted to concluding remarks.

## 2. The energy spectrum

We consider a 2D EG which we will take to lie in the Cartesian $(x, y)$ plane and which is also subjected to the following magnetic field: $\boldsymbol{B} = (B_0 + B_m(x))\hat{\boldsymbol{e}}_z$. Here the perpendicular uniform magnetic field $B_0$ is applied in the $z$-direction while $B_m(x)$, being applied also in the $z$-direction, is a unidirectional spatially modulated magnetic field which lies in the plane of the 2D EG and will be taken to be modulated along the $x$-direction. In this work we will assume a spatial magnetic modulation of the following form:

$$B_m(x) = B_m \cos(Kx) \tag{1}$$

where $K = 2\pi/a$, $a$ being the periodicity of the magnetic modulation. That is, the spatial magnetic modulation is periodic and furthermore it will be assumed to be *weak*, i.e. $B_m \ll B_0$. The single-electron Hamiltonian of the system in the effective-mass approximation is given by

$$H = \frac{1}{2m_b}(\boldsymbol{p} - e\boldsymbol{A})^2 \tag{2}$$

where $\boldsymbol{p}$ is the momentum operator, and $\boldsymbol{A}$ is the magnetic vector potential, while $e$ is the electronic charge of an electron. When the Landau gauge is chosen ($\boldsymbol{A} = (0, xB_0 + B_m/K\sin(Kx), 0)$) and exploiting the translational invariance of this Hamiltonian along the $y$-direction (such that the momentum perpendicular to the modulation, $p_y$, is conserved), by employing an envelope wavefunction of the kind

$$\Psi_{n,k_y}(x, y) = \mathrm{e}^{\mathrm{i}k_y y}\Phi_{n,k_y}(x) \tag{3}$$

the single-electron Hamiltonian given by equation (2) can be written as

$$H = H_0 + H_{B_m} \tag{4}$$

such that the envelope wavefunction can be rewritten accordingly as

$$\Psi_{n,k_y}(x, y) = \mathrm{e}^{\mathrm{i}k_y y}[\Phi^0_{n,k_y}(x) + \Phi^{B_m}_{n,k_y}(x)]. \tag{5}$$

This Hamiltonian, i.e. equation (4), is a one-dimensional Hamiltonian which describes the motion of an electron in the $x$-direction.

In equation (4) the first term is the one-dimensional Hamiltonian for a single electron in a uniform magnetic field and corresponds to the well known *Landau* system. That is,

$$H_0 = -\frac{\hbar^2}{2m_b}\frac{d^2}{dx^2} + \frac{1}{2}m_b\omega_c^2(x - x_0)^2 \tag{6}$$

where $\omega_c = eB_0/m_b$ is the cyclotron frequency and $x_0 = k_y\ell^2$ is the centre coordinate with $\ell = \sqrt{\hbar/eB_0}$ being the magnetic length and $k_y$ a quantum number corresponding to the wave vector along the *y*-direction. The corresponding normalized single-electron eigenfunctions for $H_0$ are

$$\Psi_{n,k_y}(x, y) = e^{ik_y y}\Phi^0_{n,k_y}(x) = \frac{1}{\sqrt{L_y}}e^{ik_y y}\phi_n(x - x_0) \tag{7}$$

where the $\phi_n(x - x_0)$ are the well known linear harmonic oscillator eigenfunctions centred at $x_0$ while $L_y$ is the normalization length in the *y*-direction. The associated eigenvalues for the Landau system are given by $\varepsilon_{n,k_y} = (n + 1/2)\hbar\omega_c$ which are degenerate in the quantum number $k_y$. This energy spectrum gives rise to highly degenerate and singular magnetic subbands which are referred to as Landau levels (LL).

The second term of equation (4) is given by

$$H_{B_m} = \frac{\omega_m}{K}(-\hbar k_y + eB_0x)\sin(Kx) + \frac{m_b\omega_m^2}{4K^2}(1 - \cos(2Kx)). \tag{8}$$

Here the eigenvalues and eigenfunctions corresponding to this Hamiltonian cannot be solved analytically. Instead, since we are interested only in a weak magnetic modulation, we take $H_{B_m}$ to be a small perturbation of the Landau system, $H_0$. Taking the $\Psi_{n,k_y}(x, y)$ then as the unperturbed eigenstates, one calculates from first-order perturbation theory the eigenvalues for the weakly modulated magnetic system, $H$, as

$$E_{n,k_y} = \varepsilon_{n,k_y} + V_n\cos(Kx_0) \tag{9}$$

where only terms linear in $B_m$ have been retained. Here $\varepsilon_{n,k_y} = (n + 1/2)\hbar\omega_c$, $V_n = \hbar\omega_m\left[L_n^{(1)}(\chi) - \frac{1}{2}L_n(\chi)\right]\exp(-\chi/2)$ [16], $\chi = (K\ell)^2/2$ and $L_n^{(\alpha)}(x)$ is an associated Laguerre polynomial. Note that in our case for a weak magnetic modulation the quantum numbers *n* are referred to as the *magnetic Landau band indices* and are equivalent to the LL quantum numbers *n* for the unmodulated case. This energy spectrum is no longer degenerate in the quantum number $k_y$ since $E_{n,k_y}$ is now explicitly dependent on $x_0 = k_y\ell^2$. As a result the once formerly sharp LL are broadened into bands, so-called *magnetic* Landau bands, which are of a finite width. The bandwidth for the magnetic Landau bands, which are approximately given by $2|V_n|$ in a weak spatial magnetic field modulation, are therefore dependent on the magnetic Landau band index *n* [17]. As a result, each different value of the magnetic Landau band index *n* in the energy spectrum leads to magnetic Landau bands with differing bandwidths. Thus the magnetic modulation-induced broadening of the energy spectrum is non-uniform, a feature which will be of apparent significance when it comes to an understanding of the behaviour of the dielectric response function for such a system.

It is well known that in the absence of a magnetic modulation the DOS consists of a series of delta functions at energies equal to $(n+1/2)\hbar\omega_c$. The addition of a weak spatially periodic magnetic modulation however modifies the former delta function like the DOS by broadening the singularities at the energies $(n + 1/2)\hbar\omega_c$ into bands. In this case the DOS is given by

$$D(\varepsilon) = \frac{A}{2\pi\ell^2}\sum_{n=0}^{n_{max}}\frac{\theta(V_n - |\varepsilon - (n + 1/2)\hbar\omega_c|)}{\sqrt{V_n^2 - (\varepsilon - (n + 1/2)\hbar\omega_c)^2}} \tag{10}$$

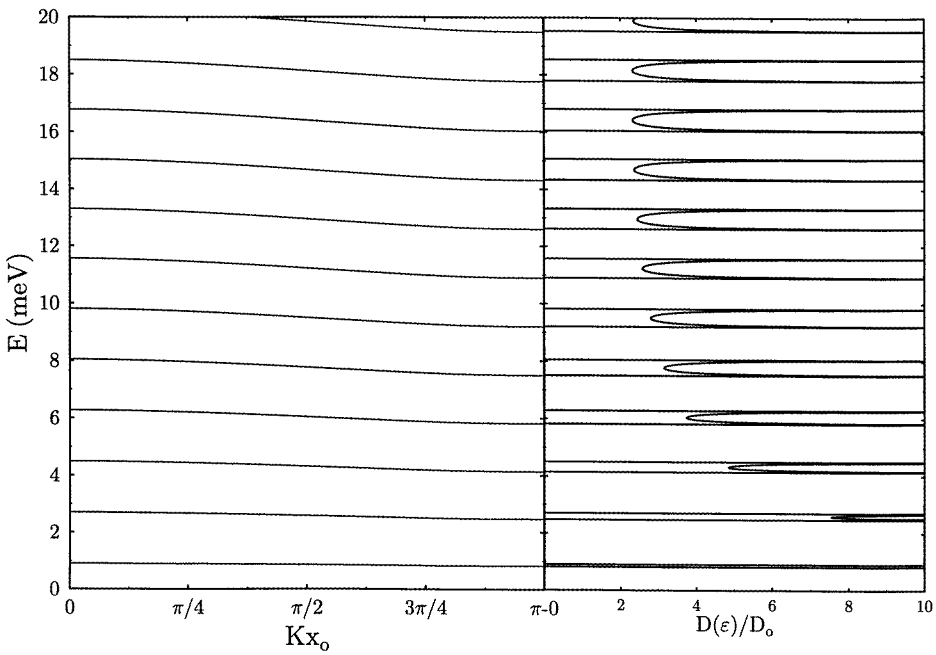


**Figure 1.** Left-hand portion: the energy spectrum due to a weak one-dimensional spatially periodic magnetic field modulation imposed on a 2D EG in a uniform perpendicular magnetic field. Here $B_m = 0.05$ T, $a = 300$ nm and $\nu = 5.5$. Right-hand portion: the corresponding DOS which has been normalized using the unbounded two-dimensional result $D_0 = Am_b/(\pi\hbar^2)$.

where $A$ is the area of the sample system, $n_{max}$ is the number of occupied magnetic Landau bands (the last magnetic band may be partially occupied) and $\theta(x)$ is the Heaviside step function. Here it can be seen that one-dimensional van Hove singularities of the inverse square-root type exist at either side of the low- and high-energy edges of the magnetic broadened Landau bands forming a double-peak structure. The energy spectrum $E_{n,k_y}$ and DOS $D(\varepsilon)$ for an additional unidirectional weakly modulated spatially periodic magnetic field imposed on a 2D EG under a uniform perpendicular magnetic field are shown in figure 1.

The chemical potential of the system is now determined through the normalization of the Fermi–Dirac distribution $f(\epsilon)$, i.e., by setting

$$N = g_s \int_0^\infty D(\epsilon) f(\epsilon)\ \mathrm{d}\epsilon \tag{11}$$

where $g_s = 2$ accounts for the spin degeneracy and $N$ is the total number of electrons. By substituting equation (10) into (11), we obtain the following closed-form expression determining the zero-temperature, magnetic-field-dependent, chemical potential $\mu$ for a 2D EG in a perpendicular magnetic field and under a unidirectional weak spatially periodic magnetic field modulation:

$$\mu(B_0, B_m, 0) = (n_{max} + 1/2)\hbar\omega_c + V_{n_{max}} \sin\left[\pi\left\{\frac{\varepsilon_F^0}{\hbar\omega_c} - (n_{max} + 1/2)\right\}\right]. \tag{12}$$

Here $\varepsilon_F^0 = \mu(0, 0, 0) = (\hbar^2/2m_b)(2\pi N/A)$ is the zero-temperature and zero-magnetic-field Fermi energy. Figure 2 shows the magnetic modulation-induced Landau fan diagram, as calculated from equation (9), for the first nine magnetic Landau bands ($n = 0, 1, \ldots, 8$). As an inset in this diagram we show the chemical potential as calculated from equation (12).

## 3. The response function

We now wish to determine the response properties of our 2D EG in a perpendicular magnetic field and under a unidirectional weak spatially periodic magnetic field modulation.

We assume that the coupling between the system and the external stimulus (an electromagnetic radiation field in the case of far-infrared spectroscopic experiments) is weak so that the response of the system is determined in terms of the properties of the system in the absence of the external stimulus i.e. a *linear* response. The response of such a system is thereby given by a dielectric response function $\varepsilon(\boldsymbol{q}, \omega)$ dependent on the frequency ($\omega$) and wave vector ($\boldsymbol{q} = (q_x, q_y)$). For our particular model system we have determined the dielectric response function within the random-phase approximation (RPA). Here we have used the unperturbed eigenstates for the Landau system, i.e. $\psi_{n,k_y}(x, y)$, as the basis set together with the first-order corrected energy spectrum $E_{n,k_y}$ as was found perturbatively in section 2. Such an approach gives a first-order corrected dielectric response function for our model system over that of the Landau system (that of a 2D EG in a perpendicular magnetic field with no spatial modulation). The RPA should be adequate provided that we confine our attention to the long-wavelength (small-wave-vector) regime since here the correlation among the electrons is quite small. It is thought that such an approach should essentially contain the most salient (new) features for such a system. More accurate calculations made in the future then should only give minor alterations to those features found within our simplified approach.

Within the RPA, the dielectric response function for our particular model system is given as

$$\epsilon(q_x, q_y, \omega) = 1 + 2\pi r_s \frac{k_F}{q} \hbar\omega_c \sum_{n,n'} C_{nn'} \sum_{x_0} \frac{f_{n',x_0+x_0'} - f_{n,x_0}}{E_{n,x_0} - E_{n',x_0+x_0'} + \hbar\omega} \tag{13}$$

where $k_F$ is the Fermi wave vector, $r_s = m_b e^2/(\hbar^2 k_F)$ is the plasma parameter, $x_0' = q_y \ell^2$, $f_{n,x_0}$ is the Fermi–Dirac distribution function and $q = \sqrt{q_x^2 + q_y^2}$ is the magnitude of the two-dimensional wave vector. It should also be understood that $\omega$ means $\omega + \mathrm{i}0^+$. The matrix element $C_{nn'}$ is given by

$$C_{nn'} = \frac{n_<!}{n_>!} X^{n_> - n_<} \mathrm{e}^{-X} [L_{n_<}^{(n_> - n_<)}(X)]^2$$

with $X = (q\ell)^2/2$, $n_> = \max(n, n')$ and $n_< = \min(n, n')$.

After separating the above equation into real and imaginary parts using the Dirac identity, it is convenient to change the centre coordinate summations to integrations over the centre coordinate via

$$\sum_{x_0} (\cdots) \to K \int_0^a (\cdots)\, \mathrm{d}x_0.$$

For the imaginary part only those $x_0$ satisfying energy conservation (enforced by the delta function) contribute. The $x_0$-integration is therefore trivial, though tedious algebraically, to evaluate. For the real part the principal-value integration is exactly solvable via a contour integral method. By choosing a new set of variables ($m = n - n'$, $n' = m'$) we obtain for the respective imaginary and real parts

$$
\begin{aligned}
\mathrm{Im}[\epsilon(q_x,q_y,\omega)] &= 2\pi^2 r_s \frac{k_F}{q}\hbar\omega_c \sum_{m=1}^{\infty}\sum_{m'=0}^{n_{max}+1} C_{m+m',m'}(f_{m+m',x_i} - f_{m',x_i+x'_0})Q_{12}^{mm'} \\
&\quad - 2\pi^2 r_s \frac{k_F}{q}\hbar\omega_c \sum_{m=1}^{\infty}\sum_{m'=0}^{n_{max}+1} C_{m+m',m'}(f_{m+m',x_j+x'_0} - f_{m',x_j})Q_{34}^{mm'} \\
&\quad + 2\pi^2 r_s \frac{k_F}{q}\hbar\omega_c \sum_{m'=0}^{n_{max}+1} \mathrm{e}^{-X}\,[L_{m'}(X)]^2\,(f_{m',x_k} - f_{m',x_k+x'_0})Q_{56}^{0m'}
\end{aligned} \tag{14}
$$

and

$$
\begin{aligned}
\mathrm{Re}[\epsilon(q_x,q_y,\omega)] &= 1 - 4\pi^2 r_s \frac{k_F}{q}\omega_c \sum_{m=1}^{\infty}\sum_{m'=0}^{n_{max}+1} C_{m+m',m'}(f_{m+m',x_i} - f_{m',x_i+x'_0}) \\
&\quad \times \frac{\theta(1-1/|\zeta_1|)}{(m\omega_c+\omega)\sqrt{1-1/\zeta_1^2}} \\
&\quad - 4\pi^2 r_s \frac{k_F}{q}\omega_c \sum_{m=1}^{\infty}\sum_{m'=0}^{n_{max}+1} C_{m+m',m'}(f_{m+m',x_j+x'_0} - f_{m',x_j})\frac{\theta(1-1/|\zeta_3|)}{(m\omega_c-\omega)\sqrt{1-1/\zeta_3^2}} \\
&\quad - 4\pi^2 r_s \frac{k_F}{q}\omega_c \sum_{m'=0}^{n_{max}+1} \mathrm{e}^{-X}\,[L_{m'}(X)]^2\,(f_{m',x_k} - f_{m',x_k+x'_0})\frac{\theta(1-1/|\zeta_5|)}{\omega\sqrt{1-1/\zeta_5^2}}.
\end{aligned} \tag{15}
$$

Here

$$
Q_{ij}^{mm'} = \frac{\theta(1-|\zeta_i|)}{\left|V_{m+m'}W_{ij} - V_{m'}\cos(Kx'_0)W_{ij} - V_{m'}\sin(Kx'_0)Z_{ij}\right|}
$$

with

$$
W_{ij} = \sqrt{(1-\zeta_i^2)/(1+\zeta_j^2)} - (\zeta_i\zeta_j)/\sqrt{1+\zeta_j^2}
$$

and

$$
Z_{ij} = \zeta_i/\sqrt{1+\zeta_j^2} + \zeta_j\sqrt{(1-\zeta_i^2)/(1+\zeta_j^2)}.
$$

The $\zeta_i$ are given as

$$
\zeta_1 = \frac{m\hbar\omega_c + \hbar\omega}{\sqrt{V_{m+m'}^2 - 2V_{m+m'}V_{m'}\cos(Kx'_0) + V_{m'}^2}} = -\zeta_3(-\omega) \qquad \zeta_5 = \frac{\hbar\omega}{2V_{m'}\sin(Kx'_0/2)}
$$

$$
\zeta_2 = \frac{V_{m'}\sin(Kx'_0)}{V_{m'}\cos(Kx'_0) - V_{m+m'}} = \zeta_4|_{m'\leftrightarrow m'+m} \qquad \zeta_6 = \frac{\sin(Kx'_0)}{\cos(Kx'_0)-1}.
$$

In equations (14) and (15), $x_\alpha$ (with $\alpha = i, j, k$), denotes the simple roots given by the set of equations $m\hbar\omega_c + V_{m+m'}\cos(Kx_\alpha) - V_{m'}\cos(Kx_\alpha + Kx'_0) \pm \hbar\omega = 0$ where the *plus* case corresponds to $i$ and $k$ (with $m = 0$ for $k$ only) and the *minus* case corresponds to $j$. We have also used Re and Im to denote the real and imaginary parts respectively. The double summations $(m, m')$ appearing in equations (14) and (15) run over all states of the system, which may either be occupied or unoccupied, and are associated physically with the intermagnetic Landau band transitions. The single summations $(m')$ appearing in equations (14) and (15) run within each singly occupied or unoccupied state of the system and are

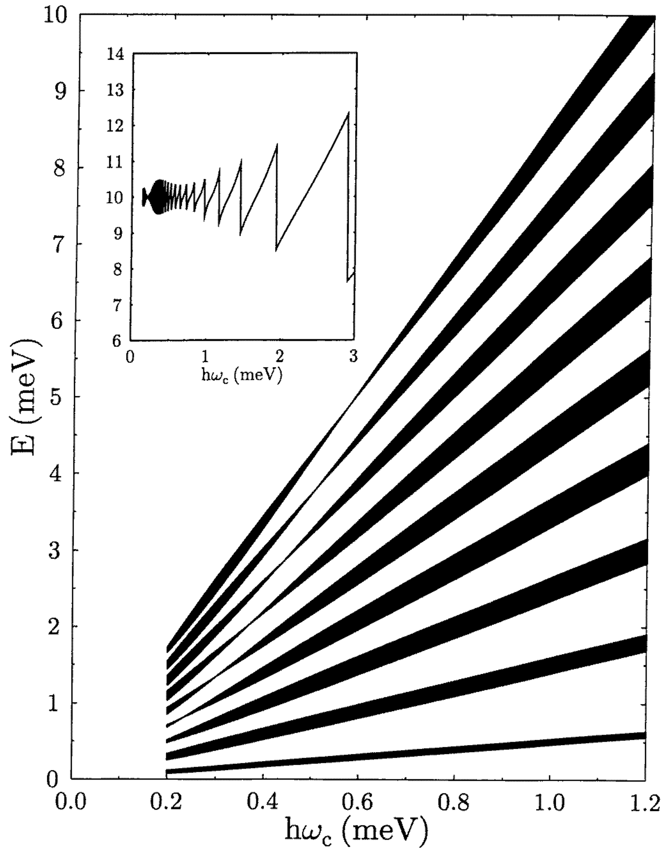


**Figure 2.** The magnetic modulation-induced Landau fan diagram for the first nine magnetic Landau bands ($n = 0, 1, \ldots, 8$). Here $B_m = 0.05$ T and $a = 300$ nm. Inset: the corresponding chemical potential as calculated from equation (12). Here we have taken $\varepsilon_F^0 = 10$ meV.

associated physically with the intramagnetic Landau band transitions. Both of the above equations are identical algebraically to those obtained by us [14] for the case of a 2D EG in a perpendicular magnetic field and under an additional unidirectional weak spatially modulated periodic *electric* potential. Equations (14) and (15) thus represent the *magnetic* analogue to the *electric* case [14]. Here however the *electric* $U$-function ($U_n = V_0 \exp(-\chi/2) L_n(\chi)$) is replaced by the *magnetic* $V$-function ($V_n$).

In all of the numerical calculations which are to follow, as an example, we have employed the following parameters which are realistic values for a typical experimental system: $B_m = 0.05$ T, $a = 300$ nm, $q = 0.2k_F$, and $q_y = 1 \times 10^6$ m$^{-1}$ at a filling factor ($\nu = \varepsilon_F^0/(\hbar\omega_c)$ and counts the number of occupied LL or Landau bands at absolute zero) of 5.5. All of the numerical calculations are performed at zero temperature and use a chemical potential $\mu$ given by equation (12). The remaining parameters used in the calculations are $\kappa = 13$ where $\kappa$ is the bulk dielectric constant of the medium, $r_s = 0.73$, and $m_b = 0.067 m_e$ where $m_e$ is the free rest mass of an electron.

Figure 3 shows typical behaviour for the imaginary part of the magnetic field-dependent RPA dielectric function in a unidirectional spatially periodic magnetic modulation which is weak. For a sufficiently small magnetic modulation amplitude $B_m$ such that the magnetic

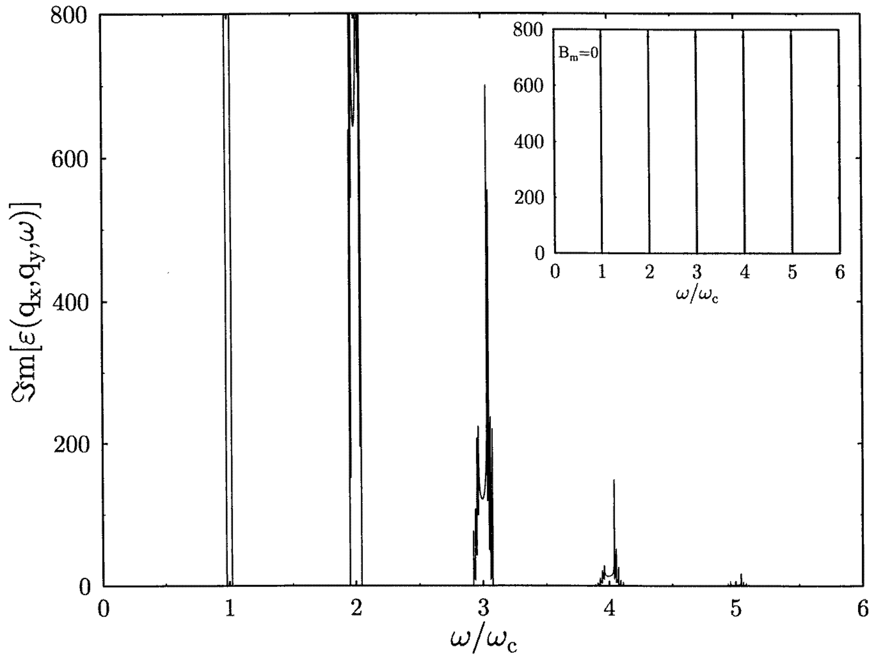


**Figure 3.** The imaginary part of the RPA dielectric function as a function of $\omega/\omega_c$ for a 2D EG in a uniform perpendicular magnetic field and in the presence of a weak one-dimensional spatially periodic magnetic field modulation. Here $B_m = 0.05$ T, $a = 300$ nm, $\nu = 5.5$ at $T = 0$ K. Other parameters used are as given in the text. Inset: the unmodulated ($B_m = 0$) case.

Landau bands do not overlap, it can be clearly seen that the imaginary part consists of a series of individually isolated double-peak structures about the resonance frequency and each of its harmonics. New subsingularities (fine structure) at either side of the band edges of each main double-peak structure are also resolved. This is to be contrasted with the unmodulated case shown as an inset in figure 3. Here the infinities are an artifact of the RPA, which neglects any intrinsic broadening of the LL. For non-integer filling factors the number of singularities on *each side* of the band edges is equal to $i + 1$ where $i$ is an integer and counts the resonance frequency (as $i = 1$) and each of its harmonics (as $i = 2, 3, 4, \ldots$), with the maximum number given by $n_{max}$. For the special case of integer filling factors this number is $i$ with the maximum number being $n_{max} - 1$. Figure 4 shows typical behaviour for the real part of the magnetic field-dependent RPA dielectric function in a unidirectional spatially periodic magnetic modulation which is weak. The real part is seen to be qualitatively very similar to the unmodulated case (shown as an inset in figure 4) except about the resonance frequency and each of its harmonics where two new features are seen to be present. The first of these features is the appearance of new subsingularities (fine structure) at the same frequencies as found in the case for the imaginary part. Again the number of such singularities on *each side* of the band edges is the same as the previously corresponding imaginary case. The second of the features is the existence of a *step region*, of finite width, about each of the resonance and harmonic frequencies, which exists between the subsingularities.

Such fine structures, although not previously reported for a weakly modulated

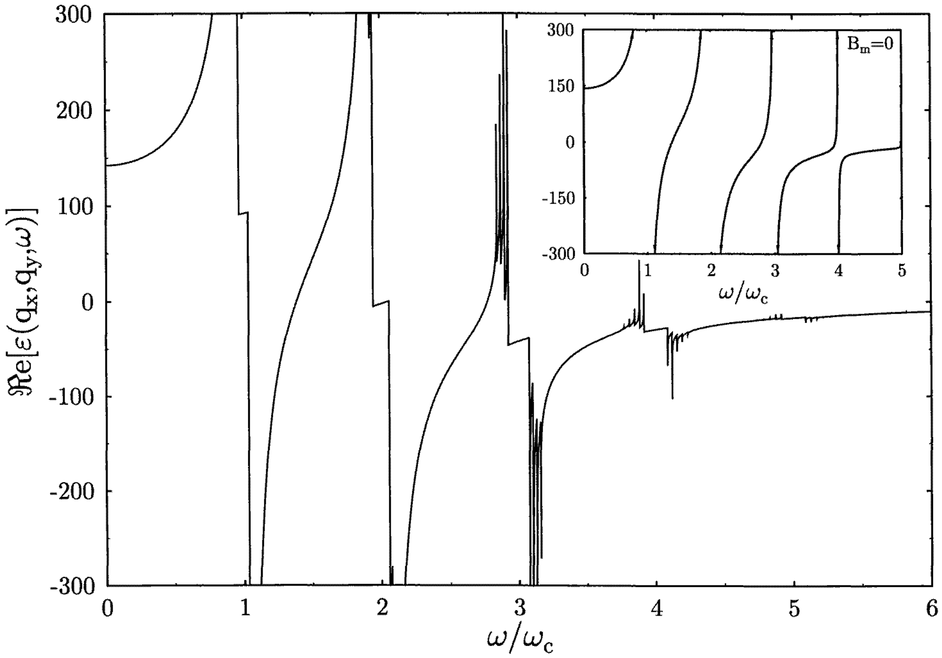


**Figure 4.** The corresponding real part to figure 3. Inset: the unmodulated ($B_m = 0$) case.

unidirectional spatial magnetic field, are however the *magnetic* analogue of those recently reported for the case of a weak unidirectional spatially modulated periodic *electric* potential [14]. Their origin is exactly analogous to the *electric* case. Here the electron–hole pair excitation for the *magnetic* case is once more significantly altered by the spatially periodic magnetic modulation. In the absence of any modulation it is well known that for infinitely sharp LL the electron–hole pair excitation can only occur at frequencies equal to the cyclotron frequency and its harmonics. The imaginary part of the dielectric response function, which describes the pair excitation, thus contains a series of highly singular delta functions at the frequencies $n\omega_c$ ($n = 1, 2, \ldots$) forming, in appearance, a so-called *Dirac comb*. The magnetic modulation-induced broadening of the energy spectrum now however leads to the reintroduction of particle–hole excitations into the dielectric response function and thus allows for pair excitations to occur within a finite frequency bandwidth around the cyclotron frequency and its harmonics. However, due to the LL broadening being non-uniform—that is dependent on the magnetic Landau band index $n$ (a feature explicitly pointed out in section 2)—each magnetic Landau band thus has a differing bandwidth and one therefore observes broadened excitations with van Hove subsingularities at the low- and high-frequency sides of the excitation peaks. This is the origin of these new subsingularities. Consider the case where the last magnetic Landau band is partially occupied (corresponding to non-integer filling factors). The allowed transitions (or particle–hole excitations) in the quantum number $n$ about $\omega \sim \omega_c$ are given by $n_{max} - 2 \rightarrow n_{max} - 1$ and $n_{max} - 1 \rightarrow n_{max}$. Each corresponding transition has two associated van Hove singularities at the band edges. Importantly however the singularities in the pair excitations for each respective transition occur over differing frequency bandwidths about the cyclotron frequency due to the $n$-dependent magnetic modulation-induced level broadening. Thus one observes a total of four singularities, two for each transition, about $\omega \sim \omega_c$. The van Hove subsingularities at the band edges are of the inverse square-root type. The number of singularities thereby increases by two as $\omega$ increases from around $n\omega_c$ to $(n+1)\omega_c$. The maximum number of singularities is however constrained to $2n_{max}$ due to the limit in initially available occupied states $n_{max}$.

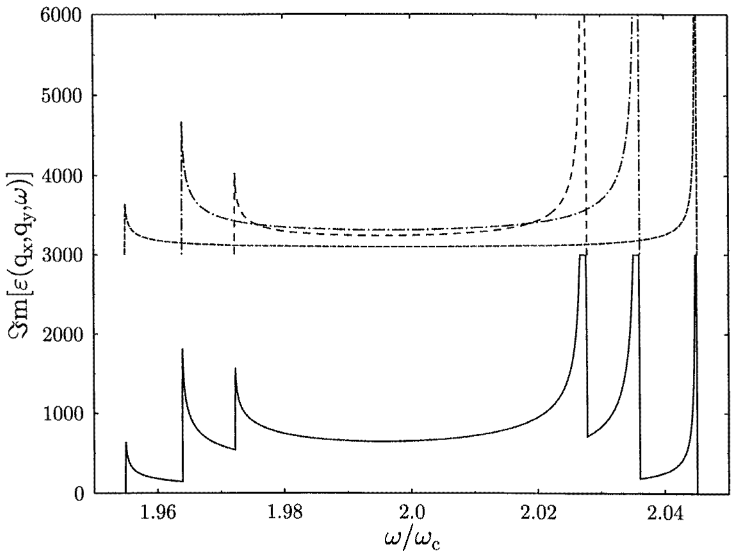


**Figure 5.** Top portion: the individual transitions between the magnetic Landau bands about $\omega \sim 2\omega_c$ for the general case of a non-integer filling factor. Here $\nu = 5.5$. The small-spaced broken line corresponds to the transition in the quantum number $n$ of $3 \rightarrow 5$, the chain line is for $4 \rightarrow 6$, while the large-spaced broken line is for $5 \rightarrow 7$. The offset is 3000 units in the $y$-direction while all other parameters used are as in figure 3. Bottom portion: the net contribution due to all three transitions showing an expected total of six van Hove subsingularities at the band edges for a non-integer filling factor about $\omega \sim 2\omega_c$.

As an illustrative example on the origin of these new subsingularities we refer the reader to figure 5. Here we consider the case in which the last magnetic Landau band is partially occupied. The allowed transitions about $\omega \sim 2\omega_c$ are: $n_{max} - 3 \rightarrow n_{max} - 1$, $n_{max} - 2 \rightarrow n_{max}$ and $n_{max} - 1 \rightarrow n_{max} + 1$. Note that for the special case where the last magnetic Landau band is completely occupied (corresponding to integer filling factors), the allowed transitions would be: $n_{max} - 2 \rightarrow n_{max}$ and $n_{max} - 1 \rightarrow n_{max} + 1$ only. Since we have considered a filling factor of $\nu = 5.5$ then in this case $n_{max} = 6$. In this particular case then one expects three singularities on either side of the band edges giving a total of six such singularities about $\omega \sim 2\omega_c$. Explicitly then the particular transitions in the quantum number $n$ involved are $3 \rightarrow 5$, $4 \rightarrow 6$ and $5 \rightarrow 7$. The individual contributions due to each of these transitions is shown in the upper portion of the figure with the resultant due to all three contributions being shown in the corresponding bottom portion. The origin and number of subsingularities are thus left in clear evidence from such a figure.

Although the structures for the *magnetic* and the *electric* modulated cases in the response function are seen to be qualitatively very similar, the sizes of their respective bandwidths can differ considerably. Such bandwidths for the subsingularities in the *magnetic* case may be up to about an order of magnitude larger compared to those seen for the *electric* case when equal modulation strengths are considered. Here by equal modulation strengths we mean $V_0 = \hbar\omega_m$, so that $|\hbar e/m_b B_m(x)| = |V_m(x)|$ where once more we have assumed a spatially periodic *electrostatic* modulation potential of the form $V_m(x) = V_0 \cos(Kx)$.

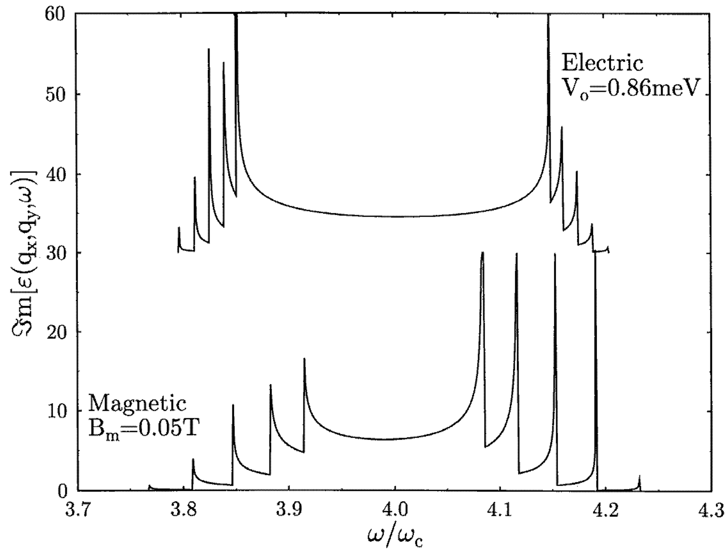


**Figure 6.** A comparison between the *electric* (top curve offset by 30 units in the *y*-direction) and *magnetic* (bottom curve) modulated cases for the imaginary part of the RPA dielectric function about $\omega \sim 4\omega_c$. Here the *electric* modulation strength is ten times that of the *magnetic* case, i.e. $V_0 = 10\hbar\omega_m$ ($B_m = 0.05$ T, $V_0 = 0.86$ meV) with all other parameters for both modulated cases remaining identical.

As noted by Peeters and Vasilopoulos [5], when only terms linear in $B_m$ are retained, the amplitude amplification in the bandwidth for the *magnetic* case, when equal modulation strengths are considered, is given by a factor of $ak_y/(2\pi)$ over that of the corresponding *electric* case. Furthermore, they also pointed out that the respective bandwidth maxima and minima are out of phase with each other by approximately 90°. So, on average, provided one is not near magnetic field values $B_0$ such that one is at or near the bandwidth minima for the *magnetic* case, such *magnetic* bandwidths will always be larger then their *electric* counterparts. Accordingly then, band-structure effects, such as the van Hove subsingularities at the band edges, for the *magnetic* case will, on average, result in stronger and more prominent features being visible as compared with the *electric* case. Such is the demonstrated case in figure 6. Here it is shown, for the case of $V_0 = 10\hbar\omega_m$, that the size of the bandwidths for the van Hove subsingularities in the response function for the *magnetic* case, in this particular example, are larger compared to their *electric* counterparts. It is therefore proposed that these new predicted fine structures due to a weak *magnetic* modulation should be more readily observed in far-infrared spectroscopy experiments than their *electric* counterparts.

## 4. Collective excitations

We now proceed to calculate the magnetoplasmon (mp) modes for our model system. These are determined by the condition that a non-zero induced charge density $\delta n$ exists for a vanishing external potential $V_{ext}$. In the RPA this condition is equivalent to the requirement that $\varepsilon(\boldsymbol{q}, \omega) = 0$. The angular frequency roots $\omega = \omega_{mp}$ of $\mathrm{Re}[\varepsilon(q_x, q_y, \omega)] = 0$ such that $\mathrm{Im}[\varepsilon(q_x, q_y, \omega_{mp})] = 0$ therefore determine the magnetoplasmon modes of the system. Using then our analytic RPA result for $\mathrm{Re}[\varepsilon(q_x, q_y, \omega)]$, i.e. equation (15), we have calculated the magnetoplasmon modes numerically.

Results here will only be given for the principal magnetoplasmon mode. We show curves for the magnetoplasmon dispersion versus wave vector $q_y$, which is parallel to the modulation direction, such that $q_x = 0$ (in which case $q = q_y$), for both an unmodulated and a weak spatial unidirectionally periodic *magnetic* field-modulated 2D EG in a perpendicular uniform magnetic field. The principal magnetoplasmon branch for both systems is such that $\omega_c \leqslant (<)\, \omega_{mp} < 2\omega_c$ ($\leqslant$ for unmodulated with $<$ for modulated) due to the presence of the uniform perpendicular magnetic field.

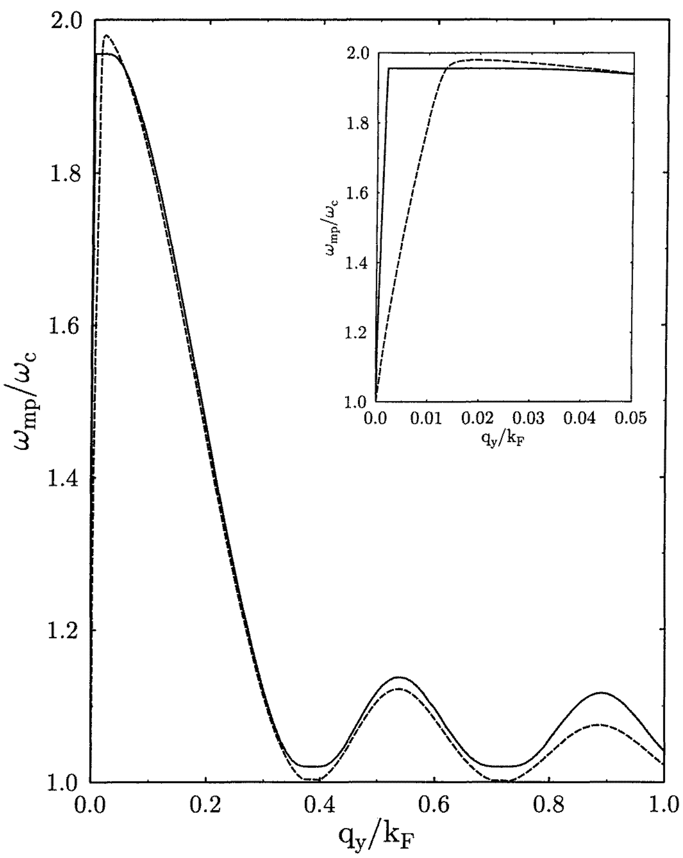


**Figure 7.** Typical behaviour for the principal magnetoplasmon mode dispersion versus wave vector $q_y$ in the case of $q_x = 0$. Here the solid line is for the weakly magnetically modulated system, $B_m = 0.05$ T and $a = 300$ nm, while the broken line is for the unmodulated case. Here we have used a filling factor of 5. The inset depicts the small-$q_y$ behaviour for each system.

For the unmodulated case the principal magnetoplasmon mode within the RPA is once more determined by the requirement that $\varepsilon(\boldsymbol{q}, \omega) = 0$. This is equivalent to finding the angular frequency root to the real part of the unmodulated dielectric function i.e. $\mathrm{Re}[\varepsilon^{Un}(q,\omega)] = 0$ such that $\mathrm{Im}[\varepsilon^{Un}(q,\omega_{mp})] = 0$. Here Un denotes the unmodulated case [18]. It is seen that the principal branch of the magnetoplasmon dispersion oscillates aperiodically with respect to $q_y$ between the frequencies $\omega_c$ to $2\omega_c$ with the minimum in the oscillation being such that $\omega_{mp} = \omega_c$. In fact if one assumes the coupling between the different magnetoplasmons modes is small such that only the lowest terms in the $m$-summation need be retained, that is the $m = 1$ term only (see equation given in reference [18]) and considering integer filling factors only, one can write, within this approximation, explicitly for the magnetoplasmon mode

$$\omega_{mp} = \omega_c \sqrt{1 + 4\pi r_s \frac{k_F}{q} \frac{X}{\nu} \mathrm{e}^{-X} [L^{(1)}_{\nu-1}(X)]^2}. \tag{16}$$

So it can be seen from the above equation that $\omega_{mp} = \omega_c$ occurs when either $q_y = 0$ or $L^{(1)}_{\nu-1}(X) = 0$. The roots of $L^{(1)}_{\nu-1}(X) = 0$ may either be obtained numerically or by the asymptotic formula for the λth zero $X^{(\alpha,n)}_\lambda \sim [\pi(\lambda - 1/4 + \alpha/2)]^2/[4(n+1/2)]$, valid for large $n$, which gives $q^\lambda_y \sim \pi(\lambda + 1/4)/\left[\ell\sqrt{2n+1}\right]$. For the particular parameters that we have chosen ($\nu = 5 \Rightarrow B_0 = 1.16$ T and thus $n = 4$) this gives $q_y/k_F \sim 0.414, 0.745, 1.076, \ldots$, together with $q_y/k_F = 0$. Such values give good agreement with those shown in figure 7 (which are: $q_y/k_F = 0, 0.386, 0.717, 1.071, \ldots$) obtained under no such approximation.

The behaviour for the magnetic spatially modulated case is thus very similar qualitatively to the unmodulated case in that the principal magnetoplasmon mode oscillates aperiodically with respect to the wave vector $q_y$ between the frequencies $\omega_c$ and $2\omega_c$. Here however the minima in the oscillations are such that $\omega_{mp} \neq \omega_c$. Such is the case since the modulation induces a broadening of the once singular behaviour in the response function about the cyclotron frequency and its harmonics (see section 3 and figures 3 and 4). As a result these so-called *step regions*, which are of finite width, in the response function correspond to a region where the imaginary part of the dielectric function is non-zero. Zeros occurring in the real part of the dielectric function in such a region correspond to modes which will be heavily damped and are therefore of no physical significance. The only stable principal mode (damping free) will thus always be situated at frequencies outside these *step regions*—that is, at frequencies greater than the cyclotron frequency and less than that of twice the cyclotron frequency. Typical behaviour for the principal magnetoplasmon dispersion versus the wave vector $q_y$, such that $q_x = 0$, for a weakly magnetically modulated system is shown in figure 7. The broken line corresponds to the unmodulated case. The inset depicts the small-$q_y$ behaviour for either system. Actually, within a small-$q_y$ approximation ($q_y \ll \sqrt{2}/\ell$), for the unmodulated case, equation (16), which determines the principal magnetoplasmons, reduces to the following well known result: $\omega^2_{mp} = \omega^2_c + \omega^2_p$ where $\omega_p = \sqrt{n_e e^2 q/(2m_b\epsilon_0\kappa)}$ is the two-dimensional plasma frequency in SI units. Here $n_e$ is the areal density of electrons while $\epsilon_0$ is the permittivity of free space. So under this approximation for the magnetically modulated system, where we have considered integer filling factors only and included only those terms such that $m = 1$ in equation (15) by assuming the coupling between the different magnetoplasmon modes is small, the principal magnetoplasmon mode will be determined by the following simple equation:

$$1 = \frac{(\hbar\omega_p)^2}{2\hbar\omega_c} \left[ \frac{1}{\sqrt{(\hbar\omega - \hbar\omega_c)^2 - \Omega^2}} - \frac{1}{\sqrt{(\hbar\omega + \hbar\omega_c)^2 - \Omega^2}} \right] \tag{17}$$

where $\Omega = 2V_{n_{max}} \sin(Kx'_0/2)$.

## 5. Summary

In conclusion we have calculated, within the RPA, the dynamical dielectric response function and collective excitations for a 2D EG in a perpendicular uniform magnetic field and in the presence of an additional weak unidirectional spatially modulated periodic *magnetic* field. It was shown that the former singular nature of the response function for the unmodulated case at the cyclotron frequencies and its harmonics is not only broadened but furthermore contains a series of subsingularities at the band edges. Such features represent the *magnetic* analogue to those recently reported for the *electric* case. Significantly however, such subsingularities at the band edges due to the magnetic modulation differ from their *electric* counterpart since the former may be up to about an order of magnitude larger in bandwidth for equal modulation strengths (i.e. $V_0 = \hbar\omega_m$) due to an amplification in amplitude of the bandwidths in the *magnetic* case. These subsingularities should therefore be more readily observed in far-infrared spectroscopy experiments than their *electric* counterparts.

For the collective excitations we show only the principal magnetoplasmon dispersion which is calculated along a direction parallel to the modulation and compare the result to the unmodulated system. The result shows the principal magnetoplasmon oscillates aperiodically with respect to the wave vector $q_y$, between the frequencies $\omega_c$ to $2\omega_c$, such that the oscillation minima are now shifted above the cyclotron frequency. The result for the small-$q$ behaviour is also explicitly given.

## Acknowledgments

Many thanks to D J Fisher and W Xu for helpful discussions. This work is supported in part by the Australian Research Council and by the University of Wollongong Postgraduate Fellowship.

## References

[1] Yoshioka D and Iye Y 1987 *J. Phys. Soc. Japan* **56** 448
[2] Vasilopoulos P and Peeters F M 1990 *Superlatt. Microstruct.* **7** 393
[3] Xue Deng Ping and Xiao Gang 1992 *Phys. Rev.* B **45** 5986
[4] Wu Xiaoguang and Ulloa Sergio E 1992 *Solid State Commun.* **82** 945
[5] Peeters F M and Vasilopoulos P 1993 *Phys. Rev.* B **47** 1466
[6] Yagi R and Iye Y 1993 *J. Phys. Soc. Japan* **62** 1279
[7] Oakeshott R B S and MacKinnon A 1993 *J. Phys.: Condens. Matter* **5** 9355
[8] Izawa S, Katsamoto S, Endo A and Iye Y 1995 *J. Phys. Soc. Japan* **64** 706
Endo A, Izawa S, Katsamoto S and Iye Y 1996 *Proc. 11th Int. Conf. on the Electronic Properties of Two Dimensional Systems (Nottingham, 1995); Surf. Sci.* at press
[9] Carmona H A, Geim A K, Nogaret A, Main P C, Foster T J, Henini M, Beaumont S P and Blamire M G 1995 *Phys. Rev. Lett.* **74** 3009
Carmona H A, Nogaret A, Geim A K, Main P C, Foster T J, Henini M, Beaumont S P, McLelland H and Blamire M G 1996 *Proc. 11th Int. Conf. on the Electronic Properties of Two Dimensional Systems (Nottingham, 1995); Surf. Sci.* at press
[10] Ye P D, Weiss D, Gerhardts R R, Seeger M, von Klitzing K, Eberl K and Nickel H 1995 *Phys. Rev. Lett.* **74** 3013
Ye P D, Weiss D, Gerhardts R R, von Klitzing K, Eberl K and Nickel H 1996 *Proc. 11th Conf. on the Electronic Properties of Two Dimensional Systems (Nottingham, 1995); Surf. Sci.* at press
[11] For a review on the earlier work done on such a system see
Pfannkuche D and Gerhardts R R 1992 *Phys. Rev.* B **46** 12 606 and references therein
[12] Manolescu A and Gerhardts R R 1995 *Phys. Rev.* B **51** 1703
[13] Cui H L, Fessatidis V and Vasilopoulos P 1995 *Phys. Rev.* B **52** 13 765

[14] Stewart S M and Zhang C 1995 *Phys. Rev.* B **52** R17 365

[15] Stewart S M and Zhang C 1995 *Semicond. Sci. Technol.* **10** 1541

[16] It should be pointed out that there are several different but equivalent ways of writing the function $V_n$, all of which have appeared in the literature. They are $V_n(x) = \hbar\omega_m e^{-x/2}\mathcal{V}_n(x)$ where

$$\mathcal{V}_n(x) = [L_n^{(1)}(x) - \tfrac{1}{2}L_n(x)] = [\tfrac{1}{2}L_n(x) + L_{n-1}^{(1)}(x)] = \tfrac{1}{2}[L_n^{(1)}(x) + L_{n-1}^{(1)}(x)].$$

All three forms are seen to be equivalent to each other by noting the following recurrence relation for the associated Laguerre polynomials; $L_n^{(\alpha)}(x) = L_n^{(\alpha+1)}(x) - L_{n-1}^{(\alpha+1)}(x)$. Here one takes $L_{-1}^{(\alpha)}(x) = 0$.

[17] For an explicit calculation of the bandwidth of the magnetic Landau bands in a weak magnetic field modulation at the Fermi energy, see

Vasilopoulos P and Peeters F M 1990 *Superlatt. Microstruct.* **7** 393

and

Peeters F M and Vasilopoulos P 1993 *Phys. Rev.* B **47** 1466

[18] Explicitly, for the unmodulated case one has for the real part of the RPA response function

$$\mathrm{Re}[\varepsilon^{Un}(q,\omega)] = 1 + 4\pi r_s \frac{k_F}{q} \sum_{m=1}^{\infty} \sum_{m'=0}^{n_{max}} C_{m+m',m'} \frac{m\omega_c^2}{m^2\omega_c^2 - \omega^2}(f_{m'} - f_{m+m'}).$$

So the principal magnetoplasmon mode in this case is determined by solving for the angular frequency roots $\omega_{mp}$, such that $\omega_c \leqslant \omega_{mp} < 2\omega_c$, the equation $\mathrm{Re}[\varepsilon^{Un}(q,\omega)] = 0$ numerically.